

Lyapunov exponents of heavy particles in turbulence

J eremie Bec

CNRS UMR6202, Observatoire de la C te d'Azur, B.P. 4229, 06304 Nice Cedex 4, France.

Luca Biferale

Dept. of Physics and INFN, University of Rome "Tor Vergata",
Via della Ricerca Scientifica 1, 00133 Roma, Italy.

Guido Boffetta

Dip. di Fisica Generale and INFN, University of Torino,
Via Pietro Giuria 1, 10125, Torino, Italy,
and CNR-ISAC c.Fiume 4, 10133 Torino Italy.

Massimo Cencini

INFN-CNR, SMC Dipartimento di Fisica, Universit  di Roma "La Sapienza",
Piazzale A. Moro 2, I-00185 Roma, Italy and ISC-CNR Via dei Taurini 19, I-00185 Roma, Italy.

Stefano Musacchio

CNRS, INLN, 1361 Route des Lucioles, F-06560 Valbonne, France.

Federico Toschi

CNR-IAC, Viale del Policlinico 137, I-00161 Roma, Italy, and INFN,
Sezione di Ferrara, via G. Saragat 1, I-44100, Ferrara, Italy.

(Dated: September 10, 2018)

Lyapunov exponents of heavy particles and tracers advected by homogeneous and isotropic turbulent flows are investigated by means of direct numerical simulations. For large values of the Stokes number, the main effect of inertia is to reduce the chaoticity with respect to fluid tracers. Conversely, for small inertia, a counter-intuitive increase of the first Lyapunov exponent is observed. The flow intermittency is found to induce a Reynolds number dependency for the statistics of the finite time Lyapunov exponents of tracers. Such intermittency effects are found to persist at increasing inertia.

Impurities suspended in incompressible flows are relevant to several physical processes, such as spray combustion, raindrop formation and transport of pollutants.^{1,2,3} These particles, being typically of finite size and heavier than the ambient fluid, cannot be modeled as simple tracers. They indeed possess inertia, which is responsible for the spontaneous generation of strong inhomogeneities in their spatial distribution.^{4,5,6} In a turbulent flow, their clustering is more efficient at small scales, below the dissipative scale, where the fluid velocity field is smooth. The intensity of particle clustering is there related to the statistics of the Lyapunov exponents of particle trajectories.⁷ The behavior of the Lyapunov exponents of inertial particles and the relation with particle clustering was recently investigated in random short-correlated flows.^{8,9,10}

In this Letter, by means of high-resolution direct numerical simulations, we investigate the Lyapunov spectra of inertial particles, varying their response time τ_s and the Reynolds number of the carrier turbulent flow. For τ_s larger than the Kolmogorov-scale turnover time τ_η , the presence of inertia results in a generic reduction of chaoticity: the leading Lyapunov Exponent is smaller than the one of tracers and the strongest chaotic fluctuations become less probable. Remarkably, for $\tau_s < \tau_\eta$, an increase of chaoticity is observed; this effect can be

understood in terms of the preferential concentration of particles in the high-strain regions of the flow. For fluid tracers, we observe intermittency effects on the statistics of chaotic fluctuations: the Reynolds-number dependence deviates from the dimensional prediction. Such deviations are found to persist for particles with inertia.

A small spherical particle of radius a with a density ρ much larger than the density ρ_0 of the surrounding incompressible fluid, evolves according to the dynamics¹¹

$$\dot{\mathbf{x}} = \mathbf{v}, \quad \dot{\mathbf{v}} = -\frac{1}{\tau_s} [\mathbf{v} - \mathbf{u}(\mathbf{x}(t), t)], \quad (1)$$

where \mathbf{u} is the fluid velocity at the location \mathbf{x} of the particle that moves with velocity \mathbf{v} , and $\tau_s = 2a^2\rho/(9\nu\rho_0)$ is the Stokes time (ν is the kinematic viscosity of the fluid). Equation (1) holds when the flow surrounding the particle is a Stokes flow; this requires $a \ll \eta$, η being the Kolmogorov scale of the flow. The Stokes number is defined as $St = \tau_s/\tau_\eta$, where τ_η is the eddy turnover time associated to η . Particles are assumed to behave passively: we neglect their feedback on the flow, which is justified for very diluted suspensions.¹² For comparison, we also study the motion of neutral particles that follow the dynamics $\dot{\mathbf{x}} = \mathbf{u}(\mathbf{x}(t), t)$, which corresponds to the limit $\tau_s \rightarrow 0$ in Eq. (1).

The incompressible fluid velocity field $\mathbf{u}(\mathbf{x}, t)$ evolves according to the Navier–Stokes equations

$$\partial_t \mathbf{u} + \mathbf{u} \cdot \nabla \mathbf{u} = -(1/\rho_0) \nabla p + \nu \Delta \mathbf{u} + \mathbf{f}, \quad \nabla \cdot \mathbf{u} = 0, \quad (2)$$

where the forcing provides an external energy input at a rate $\varepsilon = \langle \mathbf{f} \cdot \mathbf{u} \rangle$. These equations are integrated on $d = 3$ dimensional grid of size $N = 128, 256, 512$ with periodic boundary conditions, by means of a fully de-aliased pseudo-spectral parallel code with 2nd order Adams–Bashforth time-stepping. Energy is injected by keeping constant the spectral content of the two smallest wavenumber shells. Viscosity is chosen to resolve well the small-scale velocity ($k_{max}\eta \simeq 1.7$). The Reynolds numbers based on Taylor’s micro-scale is in the range $R_\lambda \in [65 : 185]$ (see Ref. 13 for further details).

Once the fluid flow has reached a statistically stationary state, particles are homogeneously seeded with initial velocities equal to the fluid velocity at their locations. We followed 33 sets of 2000 particles with Stokes numbers ranging from 0 to 2.2 for a time $\simeq 200 \tau_\eta$ after relaxation of transients.

In order to compute the Lyapunov spectrum we follow along each particle trajectory the time evolution of $2 \times d$ infinitesimal displacements in the position-velocity phase space obtained by linearizing the particle dynamics (1). The infinitesimal volume V^j , defined by j linear independent tangent vectors, grows in time with an exponential rate $\sum_{i=1}^j \gamma_i(T) = (1/T) \ln [V^j(T)/V^j(0)]$, which defines the *finite-time Lyapunov exponents* $\gamma_i(T)$ (FTLE), also called stretching rates. They asymptotically converge to the Lyapunov exponents $\lambda_i = \lim_{T \rightarrow \infty} \gamma_i(T)$, which by definition are labeled in decreasing order $\lambda_1 \geq \dots \geq \lambda_{2d}$. To compute these exponents numerically, we make use at each time lag τ_η of a standard technique based on the orthonormalization of the infinitesimal displacements by a Gram–Schmidt procedure (see, e.g., Ref. 14).

In Fig. 1 we show the behavior of the first three Lyapunov exponents as a function of St for the largest value of the Reynolds number. These three exponents rule the time evolution of infinitesimal elements in the physical space. For the range of Stokes numbers investigated here, we observe $\lambda_4 \sim \lambda_5 \sim \lambda_6 \approx -1/\tau_s$, signaling the relaxation of particle velocities to the fluid.

The largest Lyapunov exponent λ_1 measures the chaotic separation of particle trajectories. To understand how chaoticity is affected by inertia, two mechanisms have to be considered. First, inertial particles have a delay on the fluid motion; this means that their velocity is approximately given by that of tracers with a time filtering over a time window of size τ_s . This effect weakens chaoticity. Second, heavy particles are ejected from persistent vortical structures and concentrate in high-strain regions. Since these portions of the flow are characterized by larger stretching rates, the chaoticity of particle trajectories is increased with respect to tracers that homogeneously visit all the regions. As emphasized in the inset of Fig. 1 the latter effect dominates for $St < 1$ where λ_1

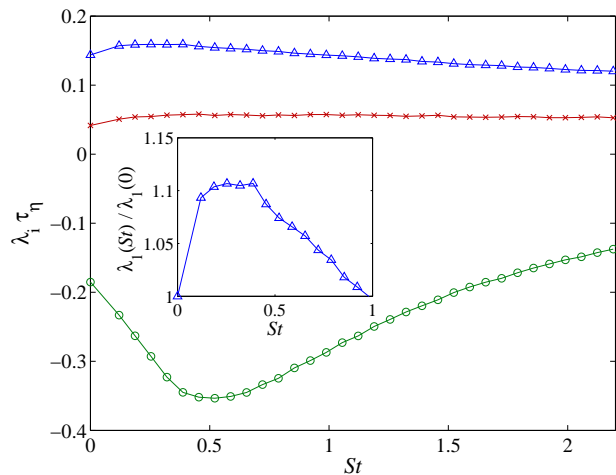


FIG. 1: Lyapunov exponents λ_i for $i = 1$ (triangles), $i = 2$ (crosses) and $i = 3$ (circles) as a function of Stokes number. $R_\lambda = 185$. In the inset we show the relative growth of the first Lyapunov exponent $\lambda_1(St)/\lambda_1(0)$ occurring at small St .

is larger than the Lyapunov exponent of the fluid tracers ($St = 0$). This is not be predicted from analytical and numerical studies done in white-in-time random velocity fields:^{9,10} such flows clearly possess no persistent structures. Conversely, at sufficiently large St , the Lyapunov exponent decreases: preferential concentration is then negligible and the time-filtering approximation becomes relevant. For such a large inertia, the white-in-time models apply and indeed predict a decrease of λ_1 as a function of St . Note that the competition between filtering and preferential concentration described above also enters in the distribution of particle acceleration.¹³

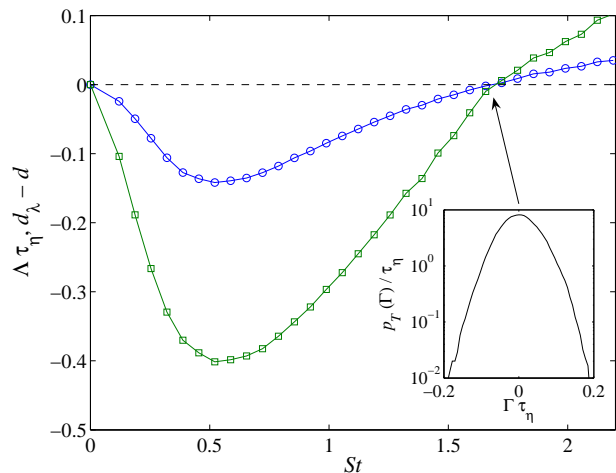


FIG. 2: Lyapunov dimension d_λ (squares) and volume growth rate $\Lambda = \sum_{i=1}^3 \lambda_i$ (circles) as a function of Stokes number ($R_\lambda = 185$). Inset: PDF of the finite-time volume growth rate $\Gamma(T)$ for $T \approx 80 \tau_\eta$.

As observed in Fig. 1, the time evolution of infinites-

imal surfaces is also affected by these two mechanisms. Indeed, at varying St , the second Lyapunov exponent λ_2 displays a behavior qualitatively similar to that of λ_1 . For the tracers ($St = 0$), incompressibility of the flow implies $\lambda_1 + \lambda_2 + \lambda_3 = 0$. Since for a time reversible dynamics one has $\lambda_2 = 0$, the ratio λ_2/λ_1 is a measure of the irreversibility of the dynamics. Previous numerical investigations at moderate Reynolds numbers¹⁵ indicate $\lambda_2/\lambda_1 \simeq 0.25$; our simulations indicate $\lambda_2/\lambda_1 = (0.28 \pm 0.02)$. This irreversibility stems from the fact that the Navier–Stokes equation itself is not invariant with respect to time reversal.

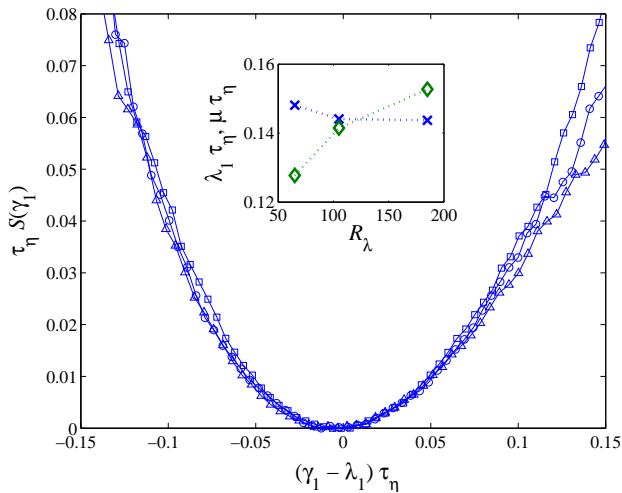


FIG. 3: Cramer function $S(\gamma_1)$ for fluid tracers for $R_\lambda = 65$ (squares), 105 (circles) and 185 (triangles). Inset: Lyapunov exponent λ_1 (crosses) and reduced variance $\mu = T\sigma^2$ (diamonds) as a function of R_λ .

The behavior of λ_3 as a function of St markedly differs from that of the first two exponents. Due to the dissipative nature of the inertial particle dynamics, volumes in physical space are not conserved. Indeed, the volume growth rate, defined as $\Lambda = \lambda_1 + \lambda_2 + \lambda_3$, which identically vanishes for fluid tracers, is negative for all Stokes numbers in the range $0 < St \lesssim 1.72$ (see Fig. 2). This means that all volumes from physical space contract to zero at large times. Such clustering, which happens at scales much smaller than η , is a consequence of the convergence of particle trajectories toward a dynamically evolving (multi)fractal set.⁷ The fractal dimension of this attractor can be estimated by means of the Kaplan–Yorke (or Lyapunov) dimension¹⁶ as $d_\lambda = J + \sum_{i=1}^J \lambda_i / |\lambda_{J+1}|$ where J is the largest integer such that $\sum_{i=1}^J \lambda_i > 0$. The fractal dimension of inertial particles is represented in Fig. 2 as a function of St . The minimum at $St \approx 0.5$ corresponds to maximal clustering. For $St \gtrsim 1.72$ the fractal dimension becomes greater than $d = 3$, indicating that the spatial distribution of particles is not fractal anymore. For $St \approx 1.72$ the volume growth rate Λ vanishes, meaning that the dynamics of such particles preserve volumes on average. However, the finite-time

volume growth rate $\Gamma = \gamma_1 + \gamma_2 + \gamma_3$ experiences large fluctuations, as shown in the inset of Fig. 2. As a result, strong local inhomogeneities are present in the particle concentration also at large values of St .

We now turn to the study of the Lyapunov exponent dependence on the Reynolds number of the flow. The inset of Fig. 3 shows the first Lyapunov exponent for neutral particles (i.e. $St = 0$) as a function of R_λ . Since λ_1 is a small-scale turbulent quantity with the dimension of an inverse time, one expects $\lambda_1 \tau_\eta \simeq const$ and thus $\lambda_1 \propto R_\lambda$. However, as a consequence of the intermittent fluctuations of the velocity gradients in turbulent flows, one can predict an anomalous dependence on Reynolds number $\lambda_1 \propto R_\lambda^\alpha$ with $\alpha < 1$ ¹⁷. This implies that $\lambda_1 \tau_\eta$ decreases with Reynolds, as indeed confirmed by our simulations.

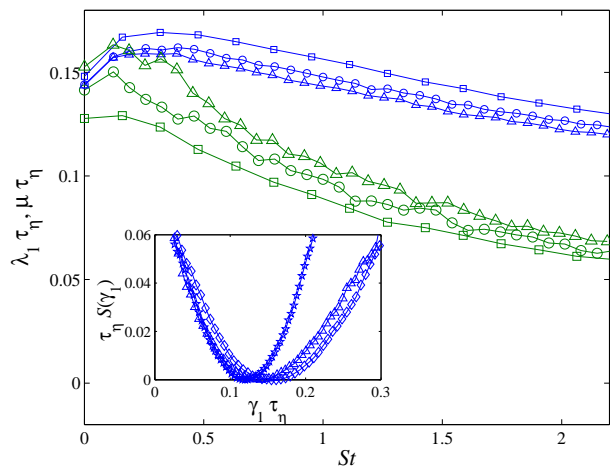


FIG. 4: Mean value λ_1 (small symbols) and reduced variance μ (large symbols) of the FTLE as a function of the Stokes number, for $R_\lambda = 65$ (squares), $R_\lambda = 105$ (circles) and $R_\lambda = 185$ (triangle). Inset: Cramer function $S(\gamma_1)$ for $R_\lambda \approx 185$, and various values of the Stokes number: $St = 0$ (triangles), $St = 0.32$ (diamonds) and $St = 2.19$ (stars).

Intermittency is actually expected to affect the whole probability distribution function (PDF) of the largest finite-time Lyapunov exponents $\gamma_1(T)$. For T sufficiently large, the distribution of FTLE is expected to obey a large-deviation principle, i.e. $p_T(\gamma_1) \propto \exp(-T S(\gamma_1))$. The Cramér (or rate) function $S(\gamma_1)$ is a non-negative concave function that vanishes at its minimum, attained for $\gamma_1 = \lambda_1$. Small fluctuations occurring when $|\gamma_1 - \lambda_1| \ll T^{-1/2}$ are described by the central-limit theorem which amounts to approximating $S(\cdot)$ by a parabola in the vicinity of its minimum. The effect of intermittency on such small fluctuations can be measured from the variance $\sigma^2 \equiv \langle (\gamma_1 - \lambda_1)^2 \rangle$ of the FTLE, or more particularly from the reduced variance $\mu = T\sigma^2$ which measures the width of the Cramér function. As predicted in Ref. 17, intermittency is responsible for an anomalous dependency of μ on the Reynolds number. More particularly $\mu \tau_\eta$ is expected to grow with R_λ . This tendency is qualita-

tively confirmed by our simulations as shown on the inset of Fig. 3. The signature of intermittency on the higher-order statistics of γ_1 can hardly be measured in a reliable way. Indeed, as shown in Fig. 3 the PDFs of γ_1 for the three R_λ considered, once centered and normalized, almost collapse for fluctuations as large as 3σ . However it is still possible to observe a systematic deviation from the Gaussian distribution. Because of incompressibility, the left tail of the PDF is bounded by the constraint that $\gamma_1 > 0$. It thus has to decrease faster than a Gaussian as indeed observed. The right part of the PDF is related to strong velocity gradients. Such events apparently lead to a tail which is fatter than Gaussian. Turbulent intermittency should therefore mainly affect the right tail.

For inertial particles, intermittent corrections act in the same direction as for fluid tracers. Figure 4 shows the behavior of λ_1 and of the reduced variance μ as a function of the Stokes number for various Reynolds numbers. As for tracers, for any given St , $\lambda_1\tau_\eta$ decreases while $\mu\tau_\eta$ increases with R_λ . The inset of Fig. 4 shows, for $R_\lambda = 185$, the Cramer function of the FTLE $\gamma_1(T)$ for both neutral particles ($St = 0$) and inertial particles with two different St . For $St < 1$, the whole distribution shifts to higher values, signaling the increased chaoticity. For $St > 1$, the distribution of FTLE shifts to lower values and fluctuations becomes less probable. The asymmetry observed in the PDF of tracer stretching rates decreases with inertia. At the largest values of St which are considered, the Cramer function γ_1 becomes indistinguishable

from a parabola. Finally, it is worth noticing that the dependence on the Reynolds number is less significant for the volume growth rate Λ , and thus for the fractal dimension. Intermittency affects only weakly particle clustering. A clearer understanding of this issue requires to investigate larger values of the Reynolds number with longer statistics. This can hardly be achieved numerically but could be done experimentally using standard box-counting techniques to estimate the fractal dimensions of the particle spatial distribution.

We have seen that two mechanisms enter the dynamics of inertial particles: they concentrate in high-strain regions and they lag behind the fluid flow. Only in either the limit of small or large inertia, one of the two effect dominates the other. At present time, tackling analytically the behavior of the largest Lyapunov exponent as a function of the Stokes number could only be done in these asymptotics.⁹ For the range of Stokes numbers considered here, both effects compete and influence the Lyapunov exponents, preventing a complete analytical description. A numerical confirmation of the present theoretical predictions would require larger computational resources.

We acknowledge useful discussions with A. Celani and A. Lanotte. This work has been partially supported by the EU under contract HPRN-CT-2002-00300 and the Galileo program on Lagrangian Turbulence. Numerical simulations have been performed at CINECA (Italy) and IDRIS (France) under the HPC-Europa program, contract number RII3-CT-2003-506079.

-
- ¹ S. Post and J. Abraham, “Modeling the outcome of drop-drop collisions in Diesel sprays,” *Int. J. Multiphase Flow* **28**, 997 (2002).
- ² G. Falkovich, A. Fouxon, and M. Stepanov, “Acceleration of rain initiation by cloud turbulence,” *Nature* **419**, 151 (2002).
- ³ J. Seinfeld, *Atmospheric Chemistry and Physics of Air Pollution* (J. Wiley and Sons, 1986).
- ⁴ J.K. Eaton and J.R. Fessler, “Preferential concentrations of particles by turbulence,” *Int. J. Multiphase Flow* **20**, 169 (1994).
- ⁵ T. Elperin, N. Kleorin and I. Rogachevskii, “Self-Excitation of Fluctuations of Inertial Particle Concentration in Turbulent Fluid Flow” *Phys. Rev. Lett.* **77**, 5373 (1996).
- ⁶ A. Pumir and G. Falkovich, “Intermittent distribution of heavy particles in a turbulent flow”, *Phys. Fluids* **16**, L47 (2004).
- ⁷ J. Bec, “Fractal clustering of inertial particles in random flows,” *Phys. Fluids* **15**, L81 (2003).
- ⁸ M. Wilkinson and B. Mehlig, “Caustics in turbulent aerosols” *Europhys. Lett.* **71**, 186 (2005).
- ⁹ K. Duncan, B. Mehlig, S. Ostlund, and M. Wilkinson, “Clustering by Mixing Flows,” *Phys. Rev. Lett.* **95**, 240602 (2005).
- ¹⁰ J. Bec, M. Cencini, and R. Hillerbrand, private communication.
- ¹¹ M.R. Maxey and J. Riley, “Equation of motion of a small rigid sphere in a nonuniform flow,” *Phys. Fluids* **26**, 883 (1983).
- ¹² J.R. Fessler, J.D. Kulick, and J.K. Eaton, “Preferential concentration of heavy particles in a turbulent channel flow,” *Phys. Fluids* **6**, 3742 (1994).
- ¹³ J. Bec, L. Biferale, G. Boffetta, A. Celani, M. Cencini, A. Lanotte, S. Musacchio, and F. Toschi, “Acceleration statistics of heavy particles in turbulence,” *J. Fluid Mech.* **550**, 349 (2006).
- ¹⁴ A. Crisanti, G. Paladin, and A. Vulpiani, *Product of random matrices*, (Springer Verlag, Berlin, 1993).
- ¹⁵ S. Girimaji and S. Pope, “Material element deformation in isotropic turbulence,” *J. Fluid Mech.* **220**, 427 (1990).
- ¹⁶ J.-P. Eckmann and D. Ruelle, “Ergodic theory of chaos and strange attractors,” *Rev. Mod. Phys.* **57**, 617 (1985).
- ¹⁷ A. Crisanti, M.H. Jensen, G. Paladin, and A. Vulpiani, “Intermittency and predictability in turbulence,” *Phys. Rev. Lett.* **70**, 166 (1993).